How much does the spatial variability of CPTu measurements affect the hydro-mechanical variables' estimation?

Vessia, Giovanna; Di Curzio, Diego; Puła, Wojciech

Important note
To cite this publication, please use the final published version (if applicable).
Please check the document version above.

How much does the spatial variability of CPTu measurements affect the hydro-mechanical variables' estimation?

Giovanna Vessia[1#,] *Diego* Di Curzio[2] and *Wojciech* Puła[3]

[1]*University "G. d'Annunzio" of Chieti-Pescara, Department of Engineering and Geology, Via dei Vestini 31, 66100 Chieti, Italy*

[2]*Delft University of Technology, Department of Water Management, Stevinweg 1, 2628 CN Delft, Netherlands*
[#]*Corresponding author:* g.vessia@unich.it
[3]*Wroclaw University of Science and Technology of Geotechnology, Department of Hydro Technology, and Underground and Hydro Engineering, Wybrzeże Wyspiańskiego 27, 50-370 Wroclaw, Poland*

ABSTRACT

Using CPTu profiles for subsoil characterisation, transformation equations must be used to obtain the hydro-mechanical properties for structures and infrastructure designing. Additionally, the uncertainty and the spatial variability of measured parameters must be taken into account for a reliable geotechnical design. In this work, we used a Stochastic Simulation approach to define reliable 3D models of two geotechnical designing variables for granular soils (friction angle–ϕ' and the Darcy permeability coefficient–k) from tip resistance (q_c), sleeve friction (f_s), and pore pressure (u_2) profiles. The selected method – the Sequential Gaussian Co-Simulation (SGCS) – provided reliable optimized 3D models of the spatial distribution of the variables of interest and allowed quantifying the propagation of the estimation uncertainty associated with the raw measurement models through the transformation equations. Overestimation (OE) and Underestimation (UE) percentages for a confidence interval of 68% were calculated throughout the 3D model: granular soils showed a larger uncertainty than fine soils concerning the measured variables (q_c, f_s, and u_2). In granular soils, the measured variable uncertainty varies up to 100% but the derived variables show different behavior: ϕ' shows UE and OE less than 25% while k reaches 100%. These differences in the propagated uncertainties depend on the transformation equations and the measured variable dependence.

Keywords: spatial variability; uncertainty propagation; CPTu readings; Sequential Gaussian Co-Simulation.

1. Introduction

The assessment of the spatial variability and uncertainty of subsoil properties is crucial for civil and environmental engineering and mining purposes. This implies that reliable subsoil models of lithotypes and hydro-mechanical variables need to be defined properly. In doing this, it must be assessed to both (1) the inherent spatial variability of natural material properties and (2) the transformation equations from measured to design variables. Both sources of uncertainties are encompassed by the propagated uncertainty (PU).

In the last forty years, several geostatistical methods have been implemented to take into account non-Gaussian distributions, co-regionalized variables, geographic trends, and external drift that come from complex 3D spatial datasets, all based on the assumption of spatial cross-correlation among measurements. This paper proposes a geostatistical simulation approach, based on the Sequential Gaussian Co-Simulation (Di Curzio et al., 2024). In this study, the PU assessment is focussed on the granular soil variable that is the friction angle ϕ', based on measured CPTu profiles (i.e., q_c, f_s, u_2). The soil behavior type Index (I_{SBT}) was also calculated to identify granular lithologies

within the studied subsoil domain. These measurements are located in a portion of Bologna district (Italy) by the Emilia Romagna Regional Office for Territorial Protection and Development (Vessia et al., 2020).

The results will be shown as estimated values and the propagated uncertainties for each variable within the 3D continuous subsoil model. Furthermore, the ϕ' propagated uncertainty will be compared with the measured variables' through the quantile analysis.

2. The multivariate stochastic simulation

In this section, the numerical method used to calculate the estimated values and the uncertainty related to the friction angle derived from CPTu profiles is illustrated. The Sequential Gaussian Co-Simulation (SGCS) method was adopted hereinafter (Gooverts 1997, Chilès and Delfiner 2012). It is the multivariate version of the Sequential Gaussian Simulation approach (SGS).

The SGCS was applied to propagate the uncertainty of ϕ' soil property, through the Linear Model of Co-regionalisation (LMC) (Journel and Huijbregts 1978). This model takes into account the multivariate spatial correlations between the study variables through a symmetric matrix of direct (diagonal) and cross (out of

diagonal) variograms (Castrignanò and Buttafuoco 2004).

In SGS, the process is repeated several times by random seeds and through different paths crossing all nodes of the simulation grid only once. As a result, several equiprobable representations of the spatial distribution of the considered variable are obtained, namely realizations, so providing a statistical distribution at each node of the grid, instead of one estimated value and the corresponding error (i.e., as in kriging methods). Owing to the assumption of Gaussian spatial behavior, the variables that do not follow the Gaussian distribution are transformed into Gaussian ones by the anamorphosis function. Then, the form of the probability distribution function is fully known, once the mean and standard deviation are determined through ordinary co-kriging.

As in this work we dealt with a multivariate case, the Kriging estimator in Eq. (1) is moved to the Co-Kriging one. In this case, the simulation relies on the fitting of a Linear Model of Coregionalization (LMC) to the matrix of all (both direct and cross-) experimental variograms of the considered variables (i.e., q_c, f_s, and u_2): (Wackernagel 2003, Castrignanò et al. 2015, Di Curzio et al. 2019, Vessia et al. 2020a, 2020b):

$$\Gamma(h) = \sum_{u=1}^{N_S} B^u g^u(h) \tag{1}$$

where g^u (h) is the spatial structure standardized to the unit sill, u is the spatial scale, B^u is the Coregionalization matrix of the LMC partial sills corresponding to the scale u, which is symmetric and semi-definite positive, $\Gamma(h)$ is the n x n matrix with direct variograms (i.e., diagonal elements) and cross-variogram (i.e., non-diagonal elements) modeled as a linear combination of N_S basic variogram functions, being NS total number of spatial scales, and h is the lag. In this study, the Linear Model of Coregionalization was fitted to the matrix of experimental direct and cross-variograms of the input data, and one thousand realizations that honor the experimental data were provided.

These realizations not only correspond to the same linear co-regionalisation model but also reproduce the same experimental histogram. In addition, their repetition provides a visual and quantitative measure of spatial uncertainty (Goovaerts 1996). Thus, these realizations through the equations of transformation gave the derived distributions of the soil properties at any point and were used to calculate some quantile values and then confidence intervals of predictions.

In this study, raw measurements of q_c, f_s, and u_2, showing skewed distributions, were transformed through Gaussian Anamorphosis (Chilès and Delfiner 2012), which consists in estimating a function converting a standardized Gaussian variable (Y) into a variable (Z=Φ(Y)), whatever its statistical distribution, through a Hermite polynomial expansion Hi(Y) truncated at a finite number of terms:

$$\Phi(Y) = \sum \Psi_i H_i(Y) \tag{2}$$

where, Ψ_i are the coefficients of the Hermite polynomials to be estimated.

Once defined the Gaussian Anamorphosis function, the transformation from a raw into the standardized gaussian variable is performed by inverting the function, as follows:

$$Y = \Phi^{-1}(Z) \tag{3}$$

The selected simulation domain has a cell size equal to 500x500x0.5 m. All the geostatistical analyses have been performed using Isatis 2018, whose results have then been visualized through Isatis.neo (www.geovariances.com/en/software/isatis-neo-geostatistics-software/).

In this paper, 1000 realizations were calculated: this number was selected based on the convergence of the total estimation variance to an approximately constant value for many simulations greater or equal to 1000.

Then, we calculated the three-dimensional expected values of both input and design variables.

3. From CPTUs to friction resistance

Starting from the set of q_c, f_s, and u_2 simulations, the soil behavior type Index I_{SBT} (Robertson 1990) has been calculated, at first.

This index enables identifying the lithological class of the investigated soil through the combination of the three variables measured with CPTUs, according to the updated equation (Robertson 2009) of the normalized index I_{SBTn}:

$$I_{SBTn} = \left[\left(3.47 - \log(Q_{tn})\right)^2 + (\log F_R + 1.22)^2\right]^{0.5} \tag{4}$$

where, $Q_{tn} = \left(\frac{q_t - \sigma_{v0}}{P_a}\right) \cdot \left(\frac{P_a}{\sigma'_{v0}}\right)^n$ is the normalized tip resistance, $F_R = \frac{f_s}{q_t - \sigma_{v0}} \cdot 100\%$ is the friction ratio, $q_t = q_c - u_2(1 - a)$, coefficient a equal to 0.8 (i.e., average value), and $n = 0.381 \cdot I_c + 0.05 \cdot \left(\frac{\sigma'_{v0}}{P_a}\right) - 0.15$, I_c is the non-normalized soil behaviour type index according to Robertson (1990), whereas σ'_{v0} and σ_{v0} are the effective and total lithostatic stresses at each depth, respectively.

The relation between I_{SBTn} values and the classes of the soil mixtures is illustrated in Table 1.

Table 1. Soil behaviour type index classes (Robertson 2009).

Soil Behavior Type	I_{SBTn}	Class
Sands – clean sand to silty sand	1.31-2.05	SBT3
Sand mixtures – silty sand to sandy silt	2.05-2.60	SBT4
Silt mixtures – clayey silt to silty clay	2.60-2.95	SBT5
Clays – silty clay to clay	2.96-3.60	SBT6

These classes were used to subsoil volume into subdomains, varying from SBT3 to SBT6.

After the I_{SBTn} was calculated, the design variables derived from the CPTU profiles were derived.

For sand-like soils (i.e., $I_{SBTn} < 2.60$), Robertson and Campanella (1983) suggested Eq. (5) to estimate the peak friction angle (ϕ', in °) for uncemented, unaged,

moderately compressible, predominately quartz sands, based on calibration chamber test results:

$$\tan(\phi') = \frac{1}{2.68}\left[\log\left(\frac{q_c}{\sigma'_{vo}}\right) + 0.29\right] \quad (5)$$

Furthermore, the hydraulic conductivity (k, in m/s) was drawn from the I_{SBTn} through the following expression:

$$k = \begin{cases} 10^{(0.952-3.04\cdot I_c)} & \text{when } 1.00 < I_{SBTn} \leq 3.27 \\ 10^{(-4.52-1.37\cdot I_c)} & \text{when } 3.27 < I_{SBTn} < 4.00 \end{cases} \quad (6)$$

it is valid for both granular and fine soils, as shown by the soil behavior type index values.

Hereinafter, we focused only on the granular soils. Thus, the propagated uncertainty of k and ϕ' were studied only in those portions of the total subsoil volume where SBT3 and SBT4 lithological classes were detected.

4. Indicators of the uncertainty propagation

To quantify the propagated uncertainty the expected values and upper (UL) and lower limits (LL) related to the confidence interval of 68% (that is the expected value plus or minus one standard deviation, σ respectively) were calculated for all the simulated and calculated variables. At this stage, the authors did not clean up data (i.e. from outliers) but considered a reduced confidence interval compared with the commonest 95%.

The LL68% and UL68% were directly calculated from the 1000 realizations of the back-transformed variables using the Anamorphosis functions previously calculated. Then, from LL and UL values, considering z(x) the estimated value of each variable at each point of the grid over the studied volume, the Underestimation (UE) and Overestimation (OE) percentages were computed, according to the following equations:

$$UE = |z(x)-LL|/(z(x))\% \quad (7)$$

$$OE = |z(x)+UL|/(z(x))\% \quad (8)$$

These parameters measure the distance between the mean of the predictions and the corresponding limits of their confidence interval at each location, providing a quantification of the local uncertainty of prediction.

Due to the high heterogeneity of the soil mixtures in the studied territory, the uncertainty propagation was analyzed within lithological subdomains, detected through the I_{SBT} index, that is $I_{SBT} < 2.6$ for granular soils, and $I_{SBT} > 2.6$ for fine soils.

Additionally, the main quantiles of the q_c, f_s, u_2, k, and ϕ' variables were listed: Q1 (25%), Q2 (50%), and Q3 (75%).

Since input and output variable estimated realizations have seldom the same units, specific indicators were defined to compare the statistical variability and assess quantitatively how the uncertainty propagates through the transformation equations. Whenever Gaussian variables are considered, the Coefficient of Variation is a descriptive measure of relative dispersion:

$$CoV = \frac{\sigma}{\mu} \quad (9)$$

where μ is the mean value of the sample. For distributions which are no-normal distributed, the coefficient of quartile variation (Zwillinger and Kokoska 2000) is define as follows:

$$CQV = \frac{Q_3-Q_1}{Q_3+Q_1} \quad (10)$$

where Q_1 and Q_3 are the 25% and 75% quartiles, respectively. This latter is a robust measure of relative dispersion especially in skewed and leptokurtic distributions (Bonett and Seier 2005).

5. Study area and dataset

The study area is located in Emilia Romagna Region (Italy), in the Po plain eastwards of Bologna, where hundreds-of-meter of alluvial deposits are present. These deposits are not layered but they are undifferentiated mixtures of sandy, gravelly, and silty-clayey soils (Fig. 1). According to ISPRA (2009a, 2009b), these deposits come from different geological bodies: the fine silty-sandy deposits belong to flooding plains, whereas coarser soils came from alluvial fans and paleo-channels. The finer deposits are lacustrine lenses. More details about the geological features of this area can be found in Vessia et al. (2020b), and Di Curzio and Vessia (2021).
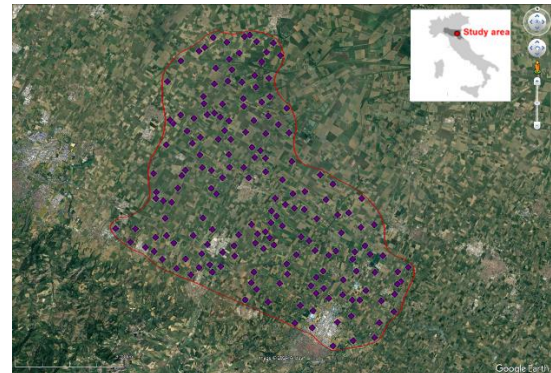

Figure 1. Map showing the location of the study area as well as the CPTUs' distribution within the selected domain.

The dataset used in this research consists of 182 CPTUs performed across an area with an extension of 900 square kilometers and investigating a volume of 92 km³ (with a depth of 30 m). These CPTu profiles have been collected in a comprehensive database by the Regional Office for Territorial Protection and Development of the Emilia-Romagna region (http://geoportale.regione.emilia-romagna.it/it), and subsequently made available by Di Curzio and Vessia (2021).

6. Results

The main features of the Linear Model of Coregionalization used in the SGCS method are listed in Tab. 2 to describe the spatial complex variability structures of the measured parameters (q_c, f_s, u_2) that were transformed into Gaussian ones by the

Anamorphosis function. A nested directional LMC was defined as consisting of a linear combination of scale-dependent variabilities: in the horizontal plane, where an isotropic variogram model was assumed, two spherical structures at two different ranges were estimated (1200 and 12000 m, respectively).

In the vertical direction, three spherical structures were included with metrical ranges and a K-Bessel function with a long-range greater than the maximum size of the study area. The presence of a local trend along the study depth is caused by the lithostatic increasing stress that influences the measured mechanical parameters. Then, the K-Bessel structure was also considered.

Table 2. Features of the Linear Model of Coregionalization (LMC) related to the Gaussian transformed variables.

Variables	Horizontal isotropic LMC structures	Range (m)
gq_c, gf_s, gu_2	Spherical	1200
	Spherical	12000
Variables	**Vertical anisotropic LMC structures**	**Range (m)**
gq_c, gf_s, gu_2	Spherical	2
	Spherical	6
	Spherical	12
	K-Bessel	>100

The SGCS approach provides 1000 three-dimensional realizations of the raw measurements and then the same number of realizations of the output variables. Figs. 2 show a 3D subsoil volume of the expected values of 1000 realizations of the back-transformed measured values.

As can be noted from Figs. 2a,b, higher estimated values of q_c and f_s correspond to a granular mixture as illustrated in Fig. 2d, through the I_{SBTn} values lower than

2.6 (see Tab.1). Granular soils are recognised in the blue area at the bottom of the subsoil model and the green ones atop and at the bottom of the 3D model.

Figs. 3a-f show the Overestimation and Underestimation percentage of the measured variables. Fine soil mixtures show much lower OE and UE values than the granular ones. The confidence interval herein chosen is the 68%, which means that 32% of the variability is not taken into account. The reason for this choice is the presence of a large number of outliers that were not eliminated a priori, and the need to study the propagation of the uncertainty by comparing measured and calculated uncertainties.

On the bottom of the model, where sandy soils are found, the q_c (Fig. 3c,d) shows an uncertainty from 75% to 100%, over and under estimations. This is caused to the larger dispersion of the tip resistance in measured profiles for coarse soils. However, on the top of the model, where the granular soils becomes finer, that is mixture of sands and silts, the uncertainty reduces and varies from 37% to 62% in both under and over estimations. The sleeve friction f_s, in Fig. 3c,d shows a lower uncertainty, varying from 37% to 62% for both UE and OE values but atop the model, some areas near the border show uncertainty as large as about 100%.

Concerning the measured pore pressure u_2, its uncertainty is almost everywhere very large (from 75% to 100%) due to the large uncertainty of these measures in soil mixtures. In three areas where silt and clays are detected, its uncertainty reduces up to 25% - 50% (Fig. 3e,f).

In Figs. 4a,b the estimated models of ϕ' and k are reported. Both variables show higher values where granular soils are detected. Taking into account only the granular soil classes SBT3 and SBT4, we can see that
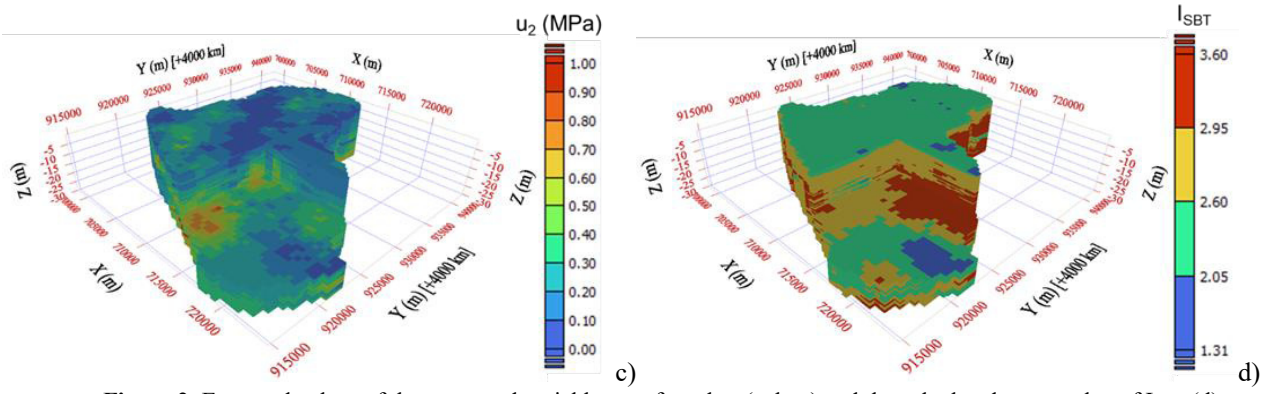

a)

b)
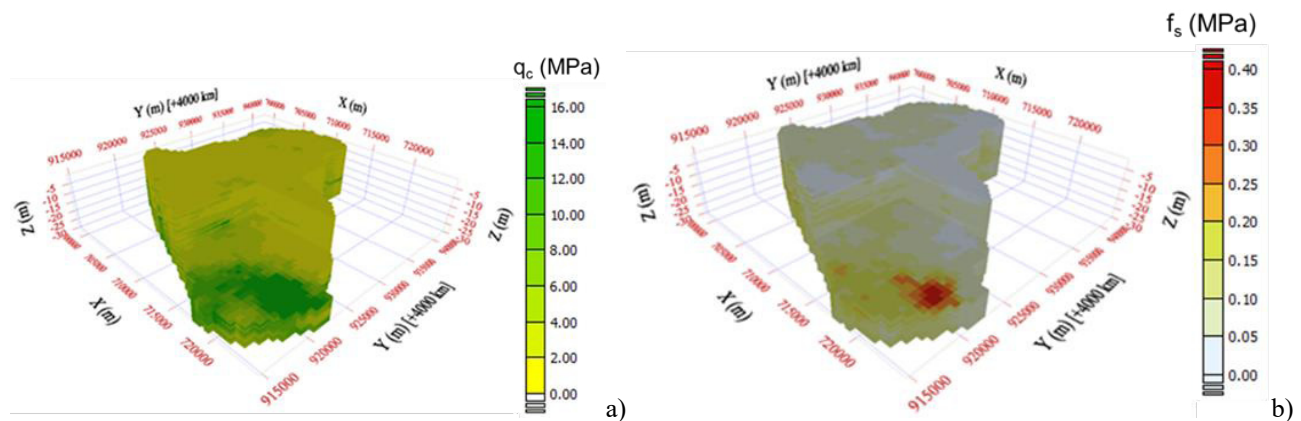
Figure 2. Expected values of the measured variables: q_c, f_s, and u_2 (a, b, c) and the calculated mean value of I_{SBTn}(d).
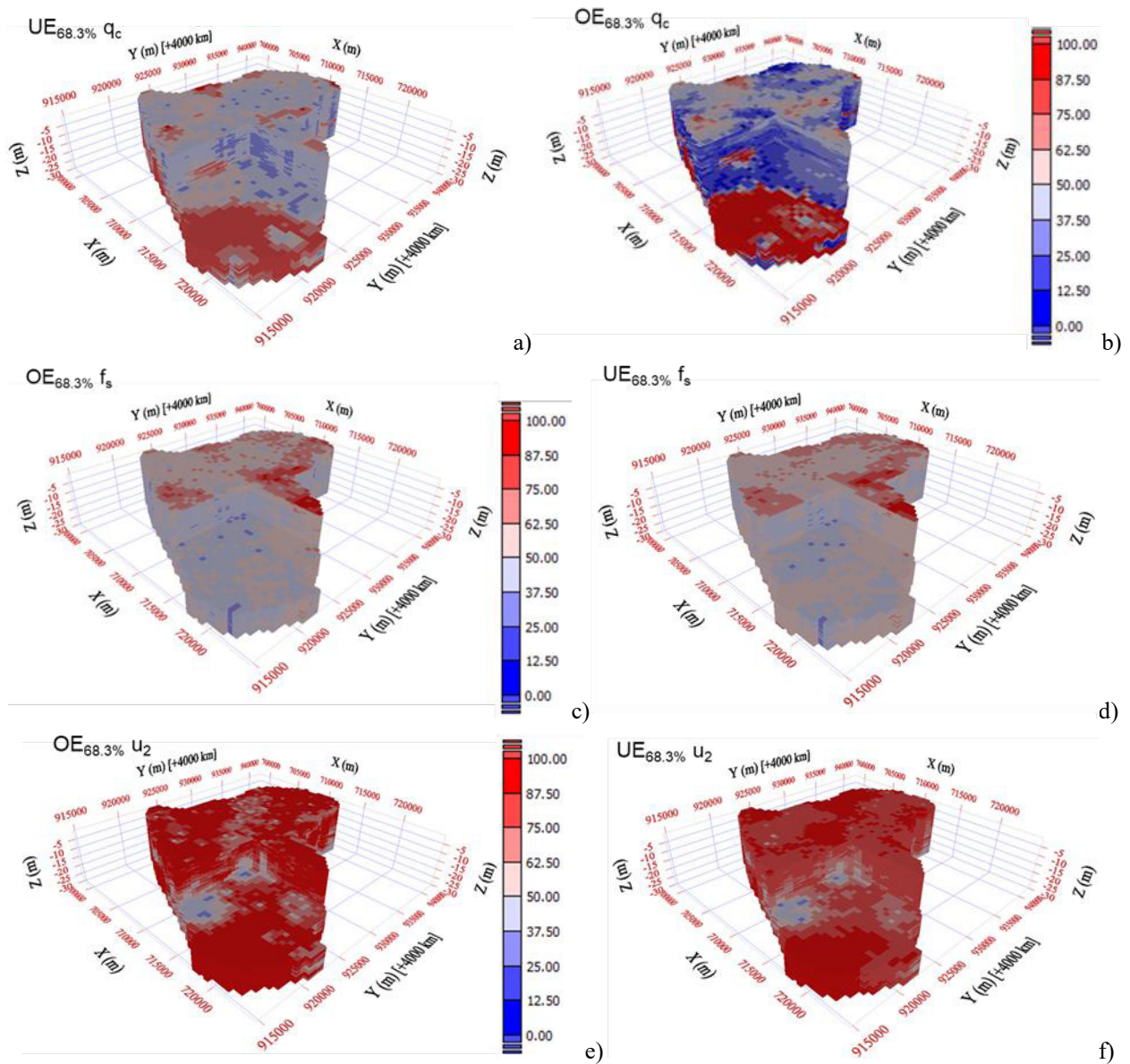

Figure 3. Overestimation and Underestimation values of the measured variables: q_c, f_s, and u_2
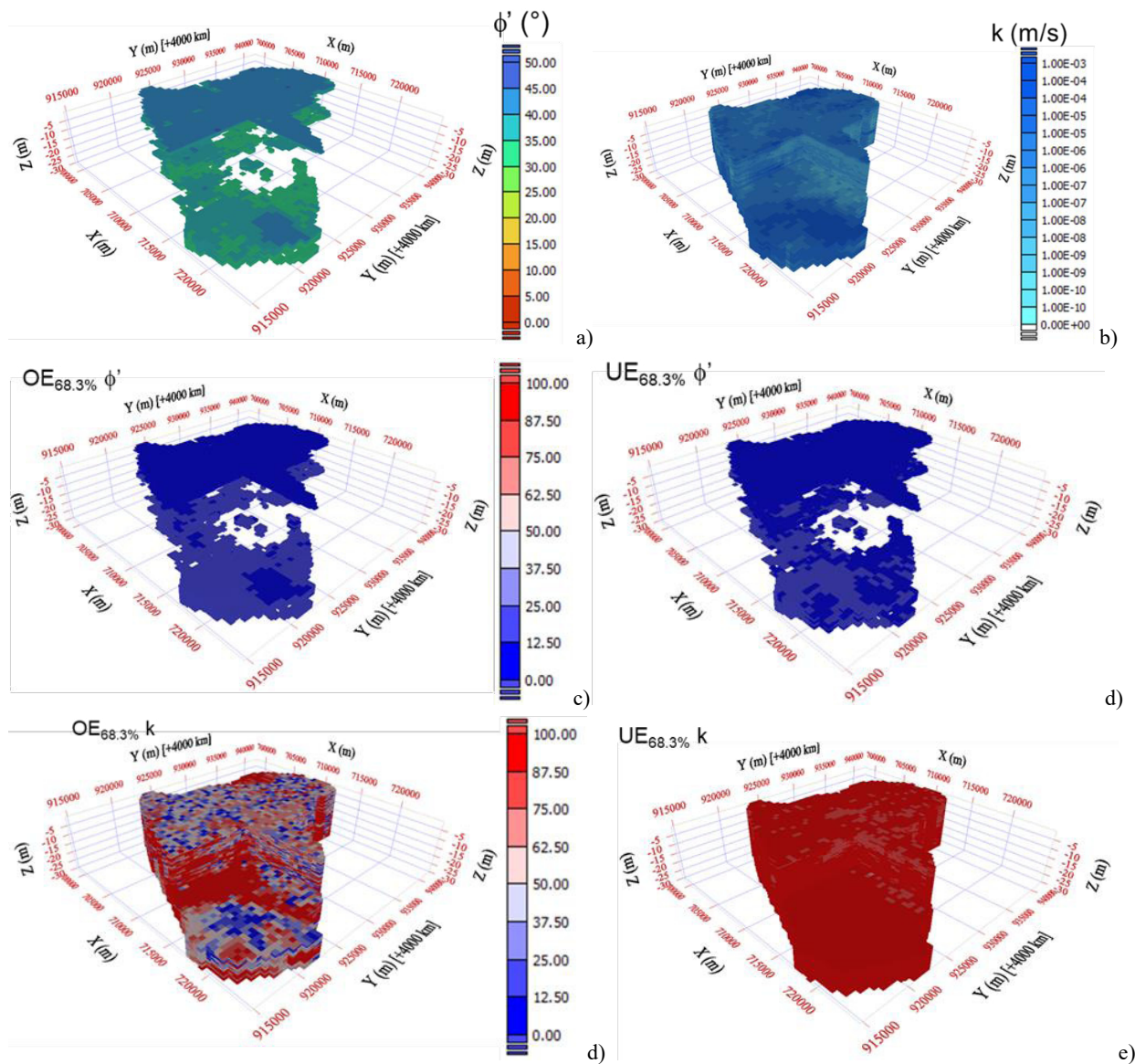
Figure 4. Expected values of the derived variables: friction angle ϕ' (a) and Darcy's coefficient k (b) and Figure 3. Overestimation and Underestimation values of ϕ' (b,c) and k (d,e).

ϕ' shows UE and OE lower than 37%. The friction angle derives from the q_c, whose uncertainty is much larger than the ϕ' one. Especially atop the model, the uncertainty falls under 12%. Such a reduction in the uncertainty depends on the calculation formula, Eq. (5). The dependence of ϕ' to the $\log(q_c)$ was responsible for this uncertainty reduction in output.

On the contrary, the Darcy coefficient k, for granular soils shows large UE values, of about 100% and less than 37% for OE values. K depends on I_c, meaning that it is a function of a complex uncertainty combination of f_s, u_2, and q_c. Additionally, k shows an asymmetric distribution towards the high values. It is calculated by two equations that do not properly depend on the granular lithological classes (see Tab. 2).

However, k values are known with a low precision, of one order of magnitude, thus 100% uncertainty, in some areas of the 3D subsoil model, can be accepted.

Table 3. Quantile indicators of the measured and calculated variables for SBT3 litho-class.

Variable	Q1	Q2	Q3	CoV	CQV
qc (MPa)	2.31	11.79	28.92	0.64	0.77
fs (MPa)	0.056	0.14	0.23	0.64	0.63
u2(MPa)	0.029	0.081	0.23	0.65	0.29
ϕ' (°)	39.93	42.83	44.46	0.047	0.04
k (m/s)	$2.7 \cdot 10^{-6}$	$1.8 \cdot 10^{-5}$	$1.4 \cdot 10^{-4}$	1.43	0.44

Finally, the uncertainty of the measured and calculated variables within the whole lithological

classes SBT3 and SBT4 was calculated in Tab. 3 and 4, through the CoV and the CQV indicators.

As shown in 4th and 5th column of Tab. 3, in sandy soils the starting uncertainty considering the subdomain is very high (about 65%) for the three input variables, while the uncertainty in terms of CoV is very high for k corresponding to 143%, while for ϕ' it is about 5%. The CQV shows lower values for u_2, ϕ', and k. This confirms the robustness of CQV against the tails where there are outliers. In this study the outliers were not eliminated, thus CQV works better than CoV to measure the propagated uncertainty.

In Tab. 4, the uncertainty of SBT4, that is the silty sand was measured. The CoV and CQV show lower values than in SBT3.

Table 4. Quantile indicators of the measured and calculated variables for SBT4 litho-class.

Variable	Q1	Q2	Q3	CoV	CQV
q_c(MPa)	1.69	2.65	28.92	0.63	0.45
fs (MPa)	0.054	0.096	0.16	0.59	0.48
u2(MPa)	0.052	0.14	0.39	0.40	0.32
ϕ' (°)	32.65	36.81	40.22	0.067	0.05
k (m/s)	$2.9 \cdot 10^{-8}$	$2.2 \cdot 10^{-6}$	$3.1 \cdot 10^{-6}$	1.01	0.61

Again, the CQV values are lower than the CoV. CQV values, in the case of ϕ', give 4% and 5%, for SBT3 and SBT4, respectively. It is very low and it is convenient compared with the laboratory measurements. Instead, k uncertainty corresponds to 100% if the tails are considered while its value reduces when CQV is calculated. This latter is 44% and 61% in SBT3 and SBT4, respectively. Then, the propagated uncertainty is shown to be less than the measured variable uncertainty when the tails of the distributions are disregarded.

The CoV, in this case of 1000 realization, can be representative of the uncertainty of the whole sample of data.

7. Conclusions

The application of the Sequential Gaussian Co-Simulation method to CPTu data through fitting a Linear Model of Coregionalization enabled us to assess the uncertainty propagation through empirical equations to derive design variables (k, and ϕ') from measured data (q_c, f_s, and u_2).

The results show:
1. for granular soils, the uncertainty propagation heavily depends mostly on the transformation expressions in granular soils;
2. ϕ' shows a very low uncertainty than q_c (5% against 64%);
3. UE and OE can be used to compare the confidence intervals of both measured and calculated variables but they are affected by the variable distribution tails;
4. CoV and CQV can be fruitfully used to describe the whole uncertainty of lithological classes.

The SGCS can be used to quantitatively assess the uncertainty propagation of other design variables but further analyses are needed to investigate the role of the outliers on the confidence intervals of the derived variables.

References

Bonett, D.G., and Seier, E. 2005. "Confidence interval for a coefficient of dispersion in nonnormal distributions", Biometrical J 48, no. 1: 144-148. https://doi.org/10.1002/bimj.200410148.

Castrignanò, A., Landrum, C., and De Benedetto, D. 2015. "Delineation of Management Zones in Precision Agriculture by Integration of Proximal Sensing with Multivariate Geostatistics", Examples of Sensor Data Fusion Agric. 80: 39-45.

Castrignano, A., and Buttafuoco, G. 2004. "Geostatistical stochastic simulation of soil water content in a forested area of south Italy", Biosyst Eng, 8, no. 2: 257-266.

Chilès, J.-P., and Delfiner, P. 2012. "Geostatistics: Modeling Spatial Uncertainty", 2nd ed., Wiley, Hoboken, NJ, USA.

Di Curzio, D., Rusi, S., and Signanini, P. 2019. "Advanced redox zonation of the San Pedro Sula alluvial aquifer (Honduras) using data fusion and multivariate geostatistics", Sci Total Environ, 695. https://doi.org/10.1016/j.scitotenv.2021.147842.

Di Curzio, D., and Vessia, G. 2021. "Multivariate Geostatistical Analysis of CPT Readings for Reliable 3D Subsoil Modeling of Heterogeneous Alluvial Deposits in Padania Plain", ISSMGE International Journal of Geoengineering Case Histories 6, no. 4: 17-34. https://doi.org/10.4417/IJGCH-06-04-02.

Di Curzio, D., Castrignanò A., Vessia, G. 2024. "Uncertainty propagation through CPTu-based hydro-mechanical subsoil models using stochastic co-simulation", submitted to Eng. Geol.

Goovaerts, P. 1996. "Stochastic simulation of categorical variables using a classification algorithm and simulated annealing", Math. Geol 28, no. 7: 909-921.

Goovaerts, P. 1997. "Geostatistics for Natural Resources Evaluation", Oxford University Press.

Isatis 2018 - https://www.geovariances.com/en/software/isatis-neo-geostatistics-software/

ISPRA, 2009a. Carta Geologica d'Italia (scala 1:50000), Foglio 221 «Bologna», Servizio Geologico d'Italia, SystemCart s.r.l, Roma.

ISPRA, 2009b. Carta Geologica d'Italia (scala 1:50000), Foglio 239 «Faenza», Servizio Geologico d'Italia, SystemCart s.r.l, Roma.

Journel, A.G., Huijbregts, C.J. 1978. "Mining Geostatistics", Academic Press, New York, NY, p. 600.

Robertson, P.K. 1990. "Soil classification using the cone penetration test", Can Geotech J 27: 151–158.

Robertson, P. K. 2009. "CPT interpretation – a unified approach", Can Geotech J 46: 1-19.

Robertson, P.K., and Campanella, R.G. 1983. "Interpretation of Cone Penetration Tests Part I (sand) Part II (clay)", Can Geotech J 20, no. 4: 719-745.

Vessia, G., Di Curzio, D., Chiaudani, A., and Rusi, S. 2020a. "Regional rainfall threshold maps drawn through multivariate geostatistical techniques for shallow landslide hazard zonation", Sci Total Environ, 70525, 135815. https://doi.org/10.1016/j.scitotenv.2019.135815

Vessia, G., Di Curzio, D., and Castrignanò, A. 2020b. "Modeling 3D soil lithotypes variability through geostatistical

data fusion of CPT parameters", Sci Total Environ, 698. https://doi.org/10.1016/j.scitotenv.2019.134340.

Wackernagel, H. 2003. "Multivariate Geostatistics: An Introduction with Applications", Springer-Verlag, Berlin.

Zwillinger, D., and Kokoska, S. 2000. "Standard probability and Statistical Tables and Formula", Chapman & Hall, Boca Raton. http://doi:10.1016/j.csda.2005.05.007

McQuerry, M. 2018. "Validation of a Clothing Heat Transfer Model in Nonisothermal Test Conditions", J Test Eval 46, no. 1: 1–7. http://doi.org/10.1520/JTE20170073

National Stone, Sand, and Gravel Association (NSSGA). 2013. "The Aggregates Handbook", 2nd ed. Englewood, CO: Society of Mining, Metallurgy, and Exploration.

Nye, J. F. 1972. "Physical Properties of Crystals". Oxford: Clarendon Press.

Oden, C. P., C. L. Ho, and H. F. Kashani. 2018. "Man-Portable Real-Time Ballast Inspection Device Using Ground-Penetrating Radar." In: Railroad Ballast Testing and Properties, edited by T. Stark, R. Swan, and R. Szecsy, 77–104. West Conshohocken, PA: ASTM International. http://doi.org/10.1520/STP160520170023

Stark, T., R. Swan, and R. Szecsy, eds. 2018. "Railroad Ballast Testing and Properties". West Conshohocken, PA: ASTM International, http://doi.org/10.1520/STP1605-EB